



Seeding fiber amplifiers with piecewise parabolic phase modulation for high SBS thresholds and compact spectra

JEFFREY O. WHITE,^{1,*} JOSHUA T. YOUNG,² CHENGLI WEI,² JONATHAN HU², AND CURTIS R. MENYUK¹

¹University of Maryland Baltimore County, 5200 Westland Blvd., Baltimore, MD 21227, USA

²Baylor University, One Bear Place #97356, Waco, Texas 76798, USA

*jow@umbc.edu

Abstract: We propose using piecewise parabolic phase modulation of the seed laser for suppressing stimulated Brillouin scattering (SBS) in a fiber amplifier. Simulations are run with a 9 m passive fiber. Compared with random phase modulation and $0-\pi$ pseudo-random phase modulation, the piecewise parabolic phase waveform yields a higher SBS threshold per unit bandwidth. If the bandwidth is defined as the range of frequencies containing 85% of the total power, the threshold for parabolic phase modulation is 1.4 times higher than the threshold for the five- or seven-bit pseudo-random modulation format. If the bandwidth is defined more tightly, e.g., the range of frequencies containing 95% of the total power, the threshold for parabolic phase modulation is three times higher. For both cases, achieving a bandwidth of 1.5 GHz requires a maximum phase shift of ~ 30 radians. All of the waveforms are compared on the basis of the bandwidth required of the phase modulator. The coherence functions are calculated in order to compare their suitability for coherent combining.

© 2019 Optical Society of America under the terms of the [OSA Open Access Publishing Agreement](#)

1. Introduction

Narrow-linewidth, high-power fiber amplifiers are needed for both coherent and incoherent beam combining or for spectral combining of multiple amplifiers. For coherent beam combining, a narrower linewidth improves combining efficiency in the presence of path length mismatch [1], allows higher angle beam steering, and enables better wavefront pre-distortion [2]. For the type of spectral beam combining in which a grating is the output coupler, a narrower linewidth reduces the output beam spreading due to diffraction. A larger number of parallel amplifiers can also be accommodated under the fiber gain spectrum, allowing higher powers to be reached. However, narrow linewidths lower the threshold for stimulated Brillouin scattering (SBS). This trade-off has led to a search for seed spectra that allow the highest threshold per unit bandwidth.

Pseudo-random bit sequence (PRBS) waveforms have a power spectrum with an envelope that is approximately sinc^2 , and random phase modulation waveforms typically have a Gaussian spectrum. Many lasers tend to exhibit a random walk in phase, leading to a Lorentzian spectrum. The optimum shape for spectral combining is rectangular. Nearly rectangular spectra can be obtained with linearly-chirped seeds with sawtooth or triangular frequency waveforms, i.e., a phase that is piecewise parabolic in time. This paper explores the suitability of chirped seeds with modulation periods in a range that covers the characteristic times given by the phonon lifetime and the fiber transit time. For a given spectral bandwidth, we will show how the threshold for sawtooth and triangular frequency waveforms depends on the period, and compare to the results for PRBS, random phase, and random-walk phase modulation.

SBS mitigation in a high-power amplifier has been achieved by engineering the fiber and by modulating the laser beam introduced into the amplifier as a seed. Random phase

modulation of a narrow band laser has been realized by applying a white noise generator to an external electro-optic phase modulator [3–6]. More recently, PRBS waveforms with π phase shifts have been extensively investigated for SBS mitigation [7,8]. A comprehensive theoretical study showed that “for a fiber length of length 9 m the patterns at or near $n = 7$ provide the best mitigation of SBS with suppression factors approaching 17 dB at a modulation frequency of 5 GHz” [9]. We will use those results as a benchmark for comparison to the waveforms we propose.

A frequency chirp of 1.2×10^{18} Hz/s has previously been used to suppress SBS in an 8.4 ns pulsed fiber amplifier [10]. A discontinuous frequency chirp (consisting of a succession of 30-MHz jumps) and a low-pass-filtered white noise source have also been used to suppress SBS in a high-gain parametric fiber amplifier [11]. A chirp with a period much longer than the fiber transit time has been used in an amplifier with a 25 m final stage to achieve a fundamental-mode pump-limited output of 1.6 kW [12]. For coherent combining, this waveform has the advantage that path length differences can be compensated with an acousto-optic frequency shifter [13]. The other significant advantage is that it is expected to yield fiber-length-independent SBS thresholds [14]. However, the techniques used to obtain μ s-ms period chirps with 1-100-nm-wide spectra [15,16] may not be applicable to the 10-100 ns period chirps with the sub-nm spectra that are desirable for spectral beam combining.

More sophisticated waveforms can be generated with a nonlinear algorithm that varies the phase at every point in time in order to minimize a cost function based on the difference between the resulting and ideal spectra [17]. The waveform can be programmed into an arbitrary waveform generator and used to drive an electro-optic modulator. This technique has been used to impress a 2-GHz-wide flat spectrum with between 16 and 380 discrete lines onto a seed, allowing amplification to 300 W [18]. Fringe visibility was also measured in a coherent combination experiment, and compared to standard- and filtered-PRBS modulation. Crosstalk between neighboring frequencies puts a limit on how closely the lines can be spaced, and thus the flatness of the spectrum. Crosstalk is not an issue with a swept-frequency source because the frequencies are not all present at the same time and position within the fiber.

The most recent work in this direction uses a model that includes the cross-interactions between spectral lines [19]. It also uses a genetic-algorithm-based Pareto multi-objective nonlinear optimization to minimize the Brillouin Stokes power and minimize the laser linewidth. The sawtooth and the triangle frequency chirp that we propose both have a phase that is piecewise parabolic in time (Fig. 1). These waveforms are comparatively simple and therefore can be generated without sophisticated algorithms and electronics.

SBS threshold for a passive fiber is commonly taken to be a ratio of 10^{-2} between the time-averaged backward Stokes power and the incident laser power, both measured at the fiber entrance ($z = 0$). For purposes of comparing different modulation formats, the exact definition of threshold should not play a large role.

Comparing spectra of different shapes requires a definition of spectral width. We define it as the range of frequencies that encompass a given fraction of the total power. (The spectra we consider are nominally symmetric, so the range will be centered on the mean frequency.) A commonly used fraction is 85%.

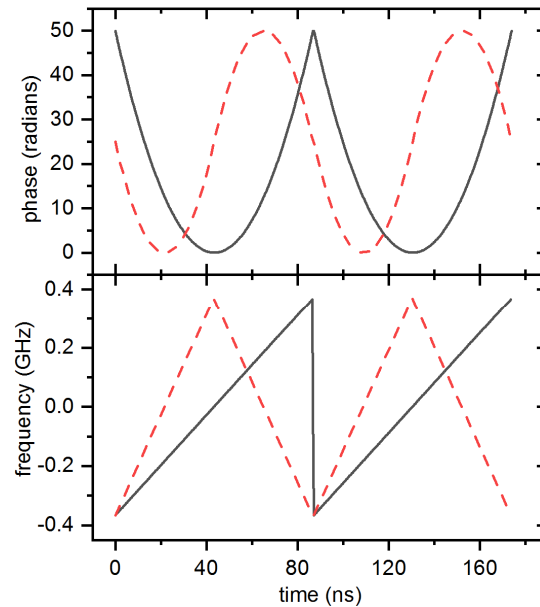


Fig. 1. Phase (above) as a function of time, and frequency (below) as a function of time for the sawtooth (solid line) and triangle (dashed line) frequency chirp.

Future systems, or different applications, e.g., close spectral packing of amplifiers, may require a tighter standard, e.g., 90% or 95%. This could also be the case for spectral beam combining systems in which the extraneous power, propagating at a large diffraction angle, causes a problem in the far field and therefore has to be dissipated internally before it reaches the exit aperture. Another consideration is how much of the light is useful when it reaches the far field or the focal plane of a lens. It is necessary to weigh whether it is more useful to have the extraneous 15% packed tightly against the other 85%, or distributed over a wide frequency range. Considerations such as these could give rise to a tighter definition of bandwidth in practice. Therefore, we consider spectral widths of 85%, 90%, and 95% power to illustrate the difference between the following spectra: Lorentzian (arising from a random phase walk), Gaussian (arising from a random phase), sinc^2 (arising from a PRBS waveform), and nearly rectangular (arising from either a sawtooth or triangular frequency chirp). We consider the case where the entire seed spectrum is incident upon the fiber, although in some experiments the extraneous spectral components could be filtered before entering the fiber.

Figure 2 shows the five spectra, normalized to have the same total power and the same 85% width. The spectrum in the fourth row is from one period of a triangle chirp waveform with the period equal to twice the transit time of a 9 m fiber, i.e., 87 ns [20]. The chirp amplitude is adjusted to give the correct 85% bandwidth. The spectrum in the fifth row is the raw Fourier transform of one period of a sawtooth chirp waveform with an 87 ns period.

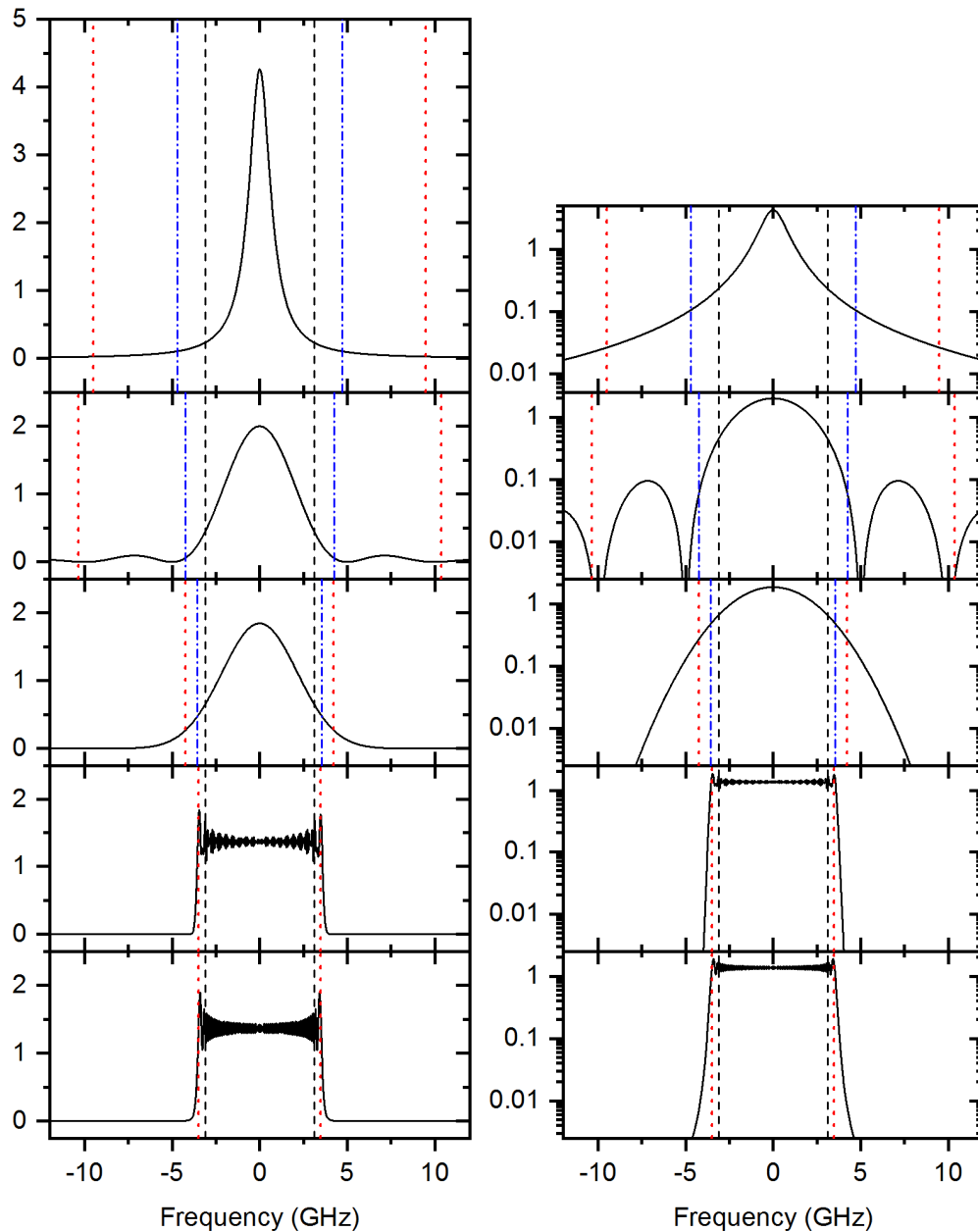


Fig. 2. Frequency spectra associated with (1st row) a random phase walk (Lorentzian), (2nd row) a $0-\pi$ generic PRBS waveform (sinc^2), (3rd row) random frequency modulation (Gaussian), (4th row) one period of a triangle chirp, and (5th row) one period of a sawtooth chirp. Plots in the left (right) column have a linear (log) vertical axis. The log scales all show three orders of magnitude variation. All spectra are normalized to have a total power of one and the same 85% width. The 90% (blue) and 95% (red) widths are also shown. The 90% width is omitted from the last rows.

Within the 85% width, the Lorentzian clearly has the most variation, the Gaussian and sinc^2 have substantially less variation, and the spectrum of the sawtooth chirp or the smoothed triangle chirp have even less. Given the nonlinear nature of the SBS, less variation in the seed spectrum raises the threshold.

As mentioned above, the spectral distribution of the out-of-band 15% also has practical implications. Spreading it over a wide range of frequencies, as with the Lorentzian and sinc^2 spectra, may lower the threshold, but also reduce by 15% the impact of the output beam at the target or sample, and create other problems. Thus there are application-specific tradeoffs to be considered, in addition to the threshold. Also shown in Fig. 2 are the 90% and 95% bandwidths. For the Lorentzian and sinc^2 spectra, these widths are substantially larger than the 85% widths, but for the rectangular spectra, they are only marginally wider.

Figure 3 shows the factor for converting from the characteristic width to the power-in-the-bucket width. As an example, for the Lorentzian, 85% of the total power is within a spectral range equal to 4.17 times the FWHM. For the sinc^2 , 85% of the power is within a range equal to 1.25 times the modulation frequency. For the Gaussian, 85% of the power is within a spectral range equal to 1.44 times the full width at $1/e$. For the sawtooth, 85% of the power is within 0.85 times the nominal bandwidth, given by the chirp times the period. Table 1 gives several of the numerical values from Fig. 3.

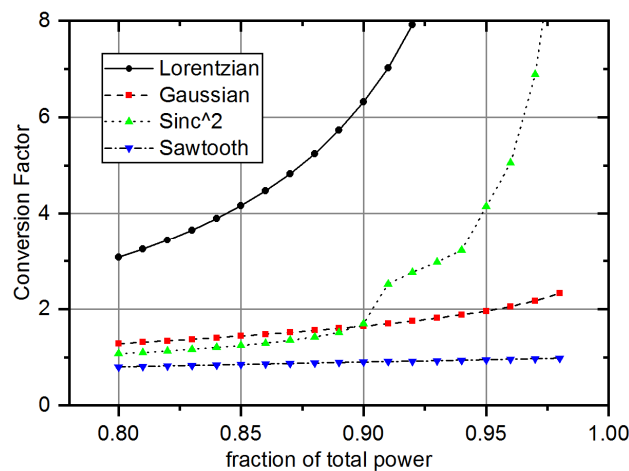


Fig. 3. Relationship between the fraction of total power contained within a spectral region and the characteristic width of the spectrum. Results are shown for the following spectra: Lorentzian, Gaussian, sinc^2 , and rectangular, produced by the phase modulation waveforms: random phase walk, random phase, PRBS, and piecewise parabolic. The characteristic widths are the Lorentzian FWHM, Gaussian FW1/e, PRBS modulation frequency, and the chirp times the period for the sawtooth. For example, 80% of the power in a Lorentzian is included in a region equal to $\sim 3 \times$ the FWHM.

Table 1. Conversion factors used in comparing various spectra

bandwidth definition	random walk	random phase	sinc^2	PRBS $n = 5$	PRBS $n = 7$	piecewise parabolic
	Lorentzian FWHM	Gaussian FW1/e	1st zero	mod. rate	mod. rate	chirp \times period
85%	4.17	1.44	1.25	1.29	1.26	0.85
90%	6.31	1.65	1.70	2.19	1.80	0.90
95%	12.7	1.96	4.15	4.46	4.38	0.95

2. Method

We model the SBS following previous treatments that solve the coupled first order equations representing propagation of the laser and Stokes wave, buildup of the acoustic wave, and initiation from a Langevin noise source representing thermal phonons throughout the length of the fiber [21]. Our code has been verified by comparison with experiments and previous theoretical work [9,12,14].

There are many parameters involved in even a basic simulation of SBS in a fiber amplifier. Some choices will favor one modulation format, other choices may favor another, so it is hard to draw universal conclusions about the relative merit. We analyze a passive fiber, and use parameters equal to those in [9], reproduced in Table 2.

Table 2. Parameters used in model

silica density	ρ_0	2201 kg/m ³	sound velocity	v_s	5.9×10^3 m/s
optical angular freq.	ω	1.77×10^{15} rad/s	fiber core area	A	7.85×10^{-11} m ²
electrostrictive constant	γ_e	1.95	Brillouin angular freq.	Ω_B	10.1×10^{10} rad/s
refractive index	n	1.5	fiber length	L	9 m
temperature	T	300 K	$2\pi \times$ phonon lifetime	$2\pi\tau$	17.5 ns

While intensity is the fundamental quantity, thresholds will be reported on the basis of power coupled into a 10 μ m core fiber, for a direct comparison to [9]. There is no transverse spatial dependence in our calculation, i.e., it is a plane wave model, a standard approximation for a fiber with only the fundamental mode present.

Our 9 m fiber length corresponds to a 7 m active fiber, which would typically absorb \sim 95% of a 976 nm pump beam, and a 2 m delivery fiber. Of course, the longitudinal dependence of the intensity in our simulation is quite different from that of an amplifier with \sim 20 dB of gain. Since gain in the active fiber adds another degree of freedom in the comparison, we model a passive fiber in this paper, consistent with [9]. The random phase modulation is achieved by low-pass filtering a white noise frequency modulation, following the analysis of [22] and using a cutoff frequency given by 0.1 times the Gaussian FW1/e.

We compare the waveforms on the basis of a 1.5 GHz seed bandwidth; the thresholds will scale linearly in this region where the seed bandwidth is much larger than the Brillouin linewidth. We investigate the 85, 90, and 95% definitions of bandwidth. The corresponding modulation rates for PRBS 5 are 1.16, 0.684, and 0.337 GHz. The corresponding modulation rates for PRBS 7 are 1.19, 0.835, and 0.342 GHz. For the PRBS 5 and 7 waveforms, the actual bandwidths differ somewhat from the generic sinc² bandwidths (see Table 1). The results shown below are obtained with a positive sawtooth chirp; the same results are obtained with a negative chirp.

We have found that running the simulation for 19 transit times, and excluding the first three transits from the averages, is sufficient to establish a threshold within a few percent of the asymptotic value (Fig. 4a). Using the PRBS waveform as an example, we sample at 64 times the modulation rate, which overestimates the threshold by only \sim 1% (Fig. 4b).

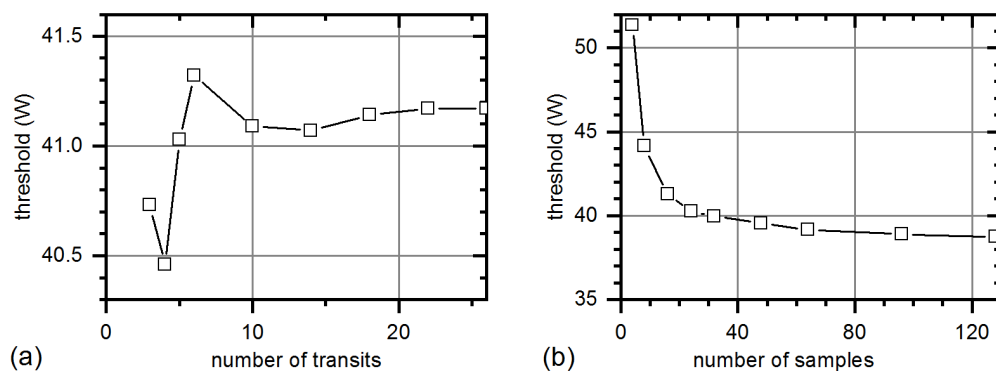


Fig. 4. (a) Threshold vs. the number of transits with 16 samples per period. (b) Threshold vs. the number of samples per period, for an average over 10 transits.

3. Results

Sixteen transits of a sawtooth frequency chirp yield a spectrum with slight peaking at the edges, some oscillations in the middle, and some wings on the side (Fig. 5a). The peaks present in the laser spectrum are exaggerated in the Stokes spectrum (Fig. 5b). A time trace of the resulting Stokes wave at threshold illustrates the random nature of the process (Fig. 5c).

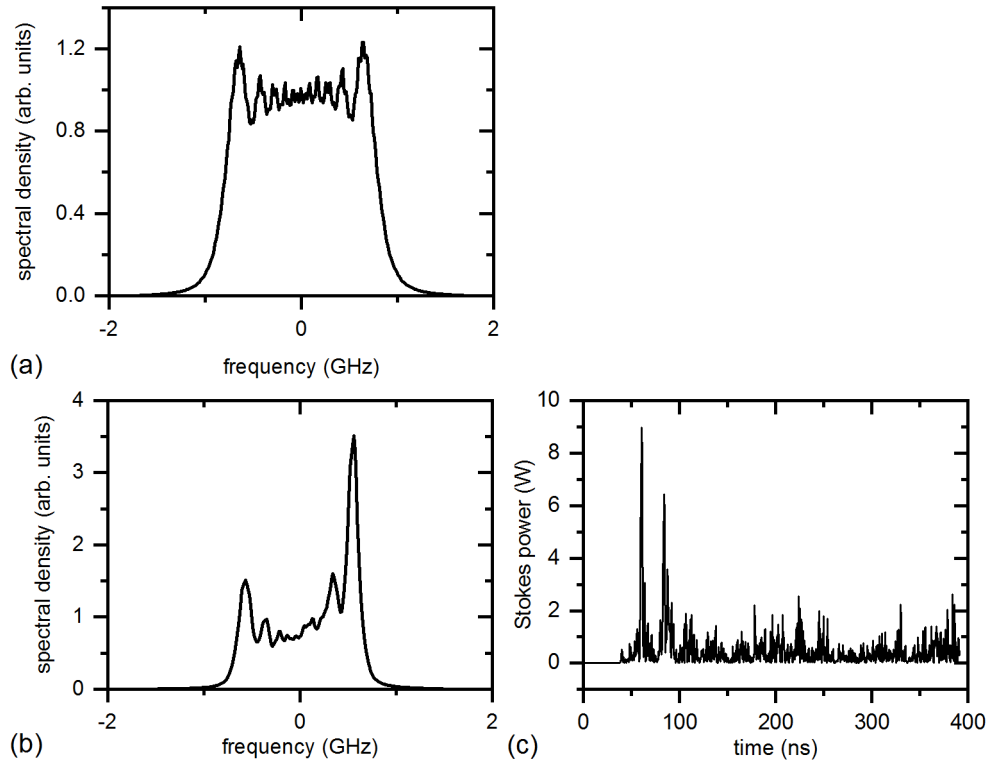


Fig. 5. (a) Spectrum of 34 periods of a 23 ns sawtooth frequency chirp. (b) Spectrum of the resulting Stokes wave at threshold. (c) Time trace of the resulting Stokes power at threshold.

As a function of incident power, the backward Stokes power increases rapidly around the threshold value, later saturating as the reflectivity approaches one. The data for six waveforms with the same 85% bandwidth are shown in Fig. 6. The sawtooth and triangle waveforms have a period of 23 ns. The thresholds are shown by the intersection with the dashed line.

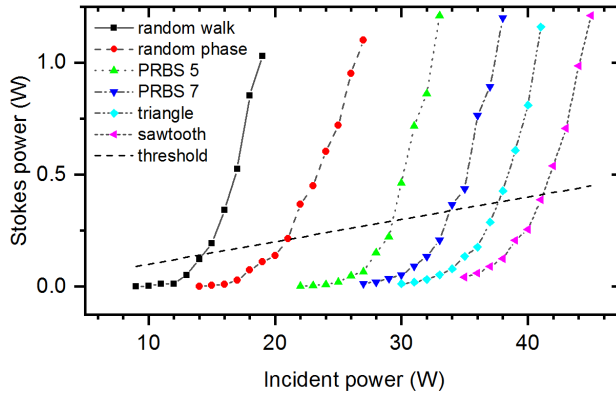


Fig. 6. Backward Stokes power vs. incident laser power for waveforms with 85% bandwidths of 1.5 GHz (left to right): random walk phase, random phase, PRBS 5, PRBS 7, triangle chirp, sawtooth chirp. The latter two have a period of 23 ns.

For a signal with a linewidth much narrower than the Brillouin linewidth and the inverse of the fiber transit time, the threshold is 2.4 W. This value will be used to normalize the other thresholds. The normalized threshold for sawtooth and triangle waveforms has a broad peak ranging from a period of $1/\Delta\nu_B = 2\pi\tau$ to twice the fiber transit time (Fig. 7). The three characteristic times are indicated with vertical lines. The thresholds for a random walk, a random phase, PRBS 5, and PRBS 7 are also shown for reference. For an 85% bandwidth equal to 1.5 GHz, the normalized threshold for the sawtooth waveform has a maximum of 16, achieved at a period of 23 ns, or $1.3/\Delta\nu_B$, and a maximum phase shift of 32 radians (Fig. 7). A second peak appears at a period of 95 ns, or $\sim 2nL/c$. No additional peaks appear at longer periods. The peak at 23 ns is of more practical interest because of the smaller required phase shifts. When compared on the basis of 85% bandwidths, the sawtooth chirp at the optimum period has a threshold 23% higher than PRBS 7, 44% higher than PRBS 5, $1.9 \times$ higher than random phase modulation, and $3.0 \times$ higher than a random walk phase.

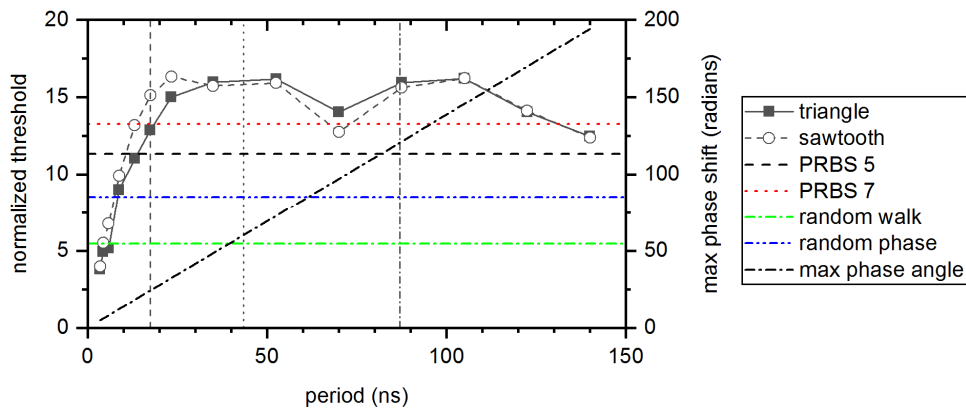


Fig. 7. Normalized threshold vs. the period, for the following waveforms: sawtooth frequency chirp, triangle frequency, PRBS 5, PRBS 7, random walk in phase, and random phase. All have an 85% bandwidth of 1.5 GHz. (Right axis) Maximum phase shift required for the chirped waveforms. Also indicated are 2π times the phonon lifetime, fiber transit time (43 ns), and round trip time.

The data for a 1.5 GHz bandwidth defined by the (tighter) 90% power criterion show a 4-6% decrease in threshold for the linear chirps, a 16-17% drop for the random walk and random phase, and a 33% decrease for the PRBS (Fig. 8). At the optimum period of 23 ns, the

sawtooth waveform has a threshold $\sim 75\%$ higher than the PRBS waveforms, and 31 radians are required. Note that the random phase and PRBS 5 have nearly the same threshold.

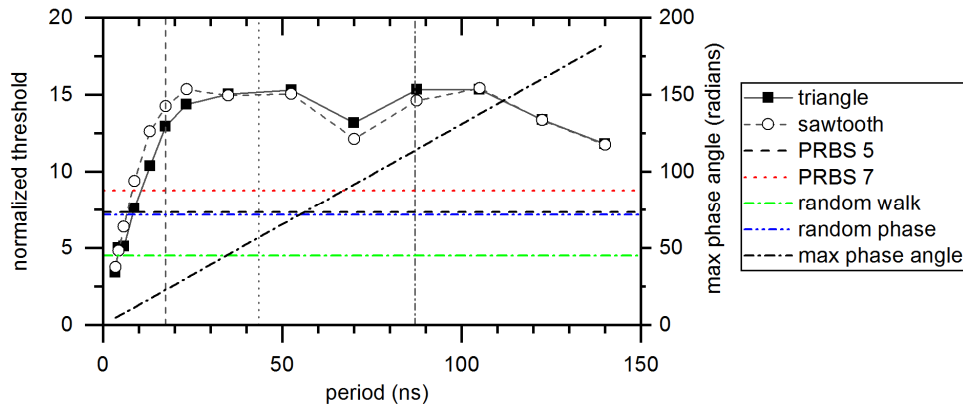


Fig. 8. Normalized threshold vs. the period for the same waveforms, with a 90% bandwidth of 1.5 GHz. (Right axis) Maximum phase shift required for the chirped waveforms.

The data for a 1.5 GHz bandwidth defined by the 95% power criterion show further small threshold decreases for the linear chirps, and large decreases for the other formats. At a period of 23 ns, the sawtooth waveform has a threshold that is $\sim 3.5 \times$ larger than the PRBS 5 waveform, and 29 radians are required. With this definition of bandwidth, the random phase modulation has a higher threshold than either of the two PRBS waveforms (Fig. 9).

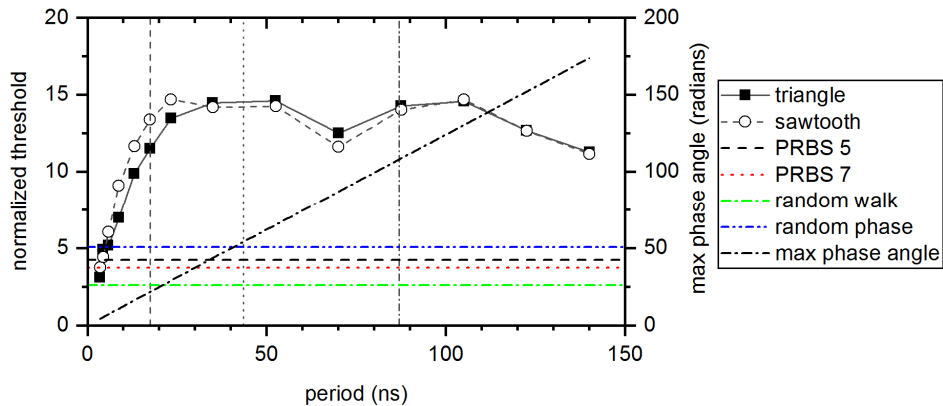


Fig. 9. Normalized threshold vs. the period for the same waveforms with a 95% bandwidth of 1.5 GHz. (Right axis) Maximum phase shift required for the chirped waveforms.

4. Discussion

For piecewise-parabolic phase waveforms, the threshold is relatively constant for periods ranging from 20 to 100 ns. The threshold decrease at long periods has a macroscopic origin. For periods longer than twice the fiber transit time, the Stokes wave originating at $z = L$ no longer encounters the entire seed bandwidth while propagating to $z = 0$. The threshold decreases at short periods because the stimulated phonons do not have time to sufficiently decay before they find themselves again in resonance with the laser-Stokes difference frequency. At short periods, the high fundamental Fourier component also means that the spectrum will be composed of harmonics spaced further apart, thus better resolved, putting more structure into the spectrum, thus lowering the threshold.

The optimal operating point for both the sawtooth and triangle waveforms is at a period of 23 ns. At this period, the maximum threshold has been achieved with a required phase shift of

~ 30 radians, which will scale linearly with bandwidth. Increasing the period increases the required phase shift without increasing the threshold. The small differences in threshold between the triangle and sawtooth waveforms are reproducible, but the choice between sawtooth and triangle may come down to practical considerations other than threshold. For an experimental realization, the triangular waveform has the advantage of no large abrupt change in phase. The sawtooth waveform has the advantage of requiring a chirp that is half as large and has only one sign.

The parabolic phase waveforms have periodic discontinuities, so it is pertinent to examine the threshold as a function of the bandwidth of the phase modulator and associated electronics, and to compare with the other waveforms. We chose the simplest response function which is a step function low-pass filter. The six waveforms in Fig. 10 all have the same 85% bandwidth of 1.5 GHz. The sawtooth and triangle have periods of 23 ns. For these conditions, the triangle and sawtooth waveforms maintain a high threshold even at cutoff frequencies $\sim 5 \times$ lower than for the PRBS waveforms.

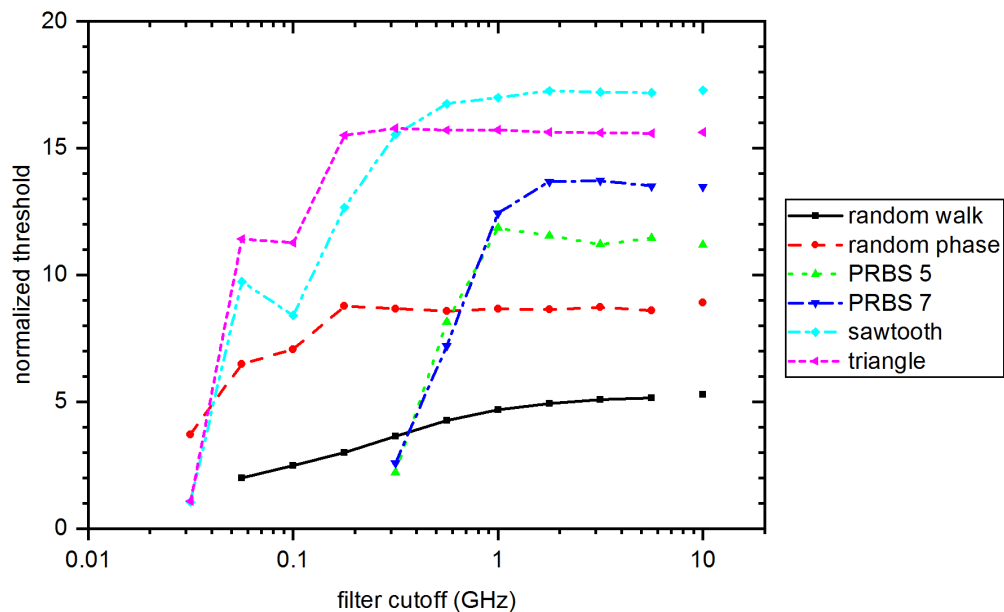


Fig. 10. Normalized threshold as a function of cutoff frequency for a low-pass filter applied to the phase waveform, for six modulation formats, all with an 85% bandwidth of 1.5 GHz. The data for no filtering is depicted at 10 GHz.

In addition to SBS threshold, optical bandwidth, and the requisite electronics bandwidth, there are or will be additional metrics for the various waveforms reflecting the suitability for coherent combining and spectral combining. For the latter, we are unaware of any additional standard metrics, and we anticipate that such metrics will be very system dependent. Regarding their suitability for coherent combining, we can compare the waveforms by calculating the complex degree of temporal coherence, given by

$$g(\tau) = \frac{\langle E^*(t)E(t+\tau) \rangle}{\langle E^*(t)E(t) \rangle}. \quad (1)$$

The real part of g decreases monotonically with time delay, τ , for some waveforms, and oscillates for others (Fig. 11). For time delays less than ~ 3 ns, the PRBS waveforms have relatively loose restrictions on path length matching, relative to the other waveforms, by virtue of having a binary waveform.

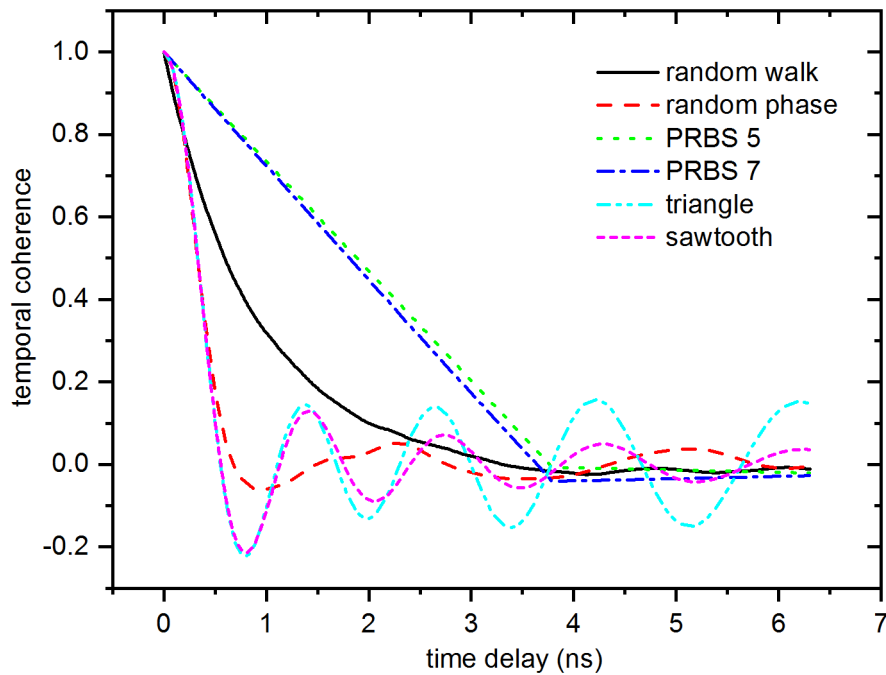


Fig. 11. The real part of the temporal coherence vs time delay, for six modulation formats in the same conditions as Fig. 10.

Future work could focus on electro-optic modulators capable of producing a 30 radian phase shift. The voltage applied to current waveguide e-o modulators is limited by the need to dissipate electrical power. Stringing multiple e-o modulators in series is limited by throughput, which is largely determined by the inefficiency of coupling the fundamental mode of the fiber pigtail to the fundamental mode of the waveguide, and vice versa. A potential solution is the lithium niobate on SiO₂ technology which allows long waveguides, CMOS-compatible driving voltages, and 70 Gbit s⁻¹ data rates [23]. An alternative to large phase shifts and piecewise parabolic waveforms with 20-30 ns periods, is to reproduce the parabola modulo 2π . This shifts the practical difficulty to generating rapid 2π phase shifts at more frequent intervals.

5. Conclusion

For fiber amplifiers, seed lasers with piecewise parabolic phase waveforms, e.g., those produced by a sawtooth or triangular linear frequency chirp, offer a significantly higher SBS threshold, compared to the conventional random phase variation, and pseudo-random waveforms. The definition of bandwidth for spectra of qualitatively different shapes is shown to have a large influence on the relative thresholds. For example, at the 85% power definition, the PRBS waveforms have a threshold superior to that of the random phase. At the 95% power definition, the random phase has a higher threshold.

The trend in spectral beam combining toward squeezing more amplifiers under the Yb gain curve will favor the nearly rectangular spectra provided by the parabolic phase waveforms. Applications where the far-out-of-bandwidth power has to be dissipated will also benefit from the relatively compact rectangular spectrum.

Compared to binary waveforms, e.g., PRBS, coherent combination with piecewise parabolic and random phase waveforms will require tighter path length matching, due to their analog nature.

Practical implementation of the piecewise parabolic waveforms will depend on the development of electro-optic modulators with adequate throughput and capable of ~ 30 radian phase shifts. Modulators producing more modest phase shifts could be used if the frequency response is sufficient to generate the same parabolic phase shift, modulo an integer multiple of 2π . If we compare the bandwidth required of the phase modulators, the piecewise parabolic waveforms require $\sim 5 \times$ less modulator bandwidth than the PRBS waveforms, for a given spectral bandwidth.

Funding

National Science Foundation (NSF) (ECCS-1809622).

Acknowledgments

Helpful discussions with Dr. David M. Brown and Dr. Andy J. Goers at Johns Hopkins Applied Physics Laboratory, and excellent suggestions from the reviewer are gratefully acknowledged.

References

1. I. Dajani, A. Flores, R. Holten, B. Anderson, B. Pulford, and T. Ehrenreich, "Multi-kilowatt power scaling and coherent beam combination of narrow-linewidth fiber lasers," *Proc. SPIE* **9728**, 972801 (2016).
2. M. Vorontsov, G. Filimonov, V. Ovchinnikov, E. Polnau, S. Lachinova, T. Weyrauch, and J. Mangano, "Comparative efficiency analysis of fiber-array and conventional beam director systems in volume turbulence," *Appl. Opt.* **55**(15), 4170–4185 (2016).
3. G. D. Goodno, S. J. McNaught, J. E. Rothenberg, T. S. McComb, P. A. Thielen, M. G. Wickham, and M. E. Weber, "Active phase and polarization locking of a 1.4 kW fiber amplifier," *Opt. Lett.* **35**(10), 1542–1544 (2010).
4. A. Mussot, M. Le Parquier, and P. Szriftgiser, "Thermal noise for SBS suppression in fiber optical parametric amplifiers," *Opt. Commun.* **283**(12), 2607–2610 (2010).
5. C. X. Yu, S. J. Augst, S. M. Redmond, K. C. Goldizen, D. V. Murphy, A. Sanchez, and T. Y. Fan, "Coherent combining of a 4 kW, eight-element fiber amplifier array," *Opt. Lett.* **36**(14), 2686–2688 (2011).
6. V. R. Supradeepa, "Stimulated Brillouin scattering thresholds in optical fibers for lasers linewidth broadened with noise," *Opt. Express* **21**(4), 4677–4687 (2013).
7. D. Brown, M. Dennis, and W. Torruellas, "Improved phase modulation for SBS mitigation in kW-class fiber amplifiers," presented at SPIE Photonics West, San Francisco, CA (January 24, 2011).
8. A. Flores, T. Ehrenreich, R. Holten, B. Anderson, and I. Dajani, "Multi-kW coherent combining of fiber lasers seeded with pseudo random phase modulated light," *Proc. SPIE* **9728**, 97281Y (2016).
9. C. Zeringue, I. Dajani, S. Naderi, G. T. Moore, and C. Robin, "A theoretical study of transient stimulated Brillouin scattering in optical fibers seeded with phase-modulated light," *Opt. Express* **20**(19), 21196–21213 (2012).
10. P. I. Ionov and T. S. Rose, "SBS reduction in nanosecond fiber amplifiers by frequency chirping," *Opt. Express* **24**(13), 13763–13777 (2016).
11. B. Coles, B. P.-P. Kuo, N. Alic, S. Moro, C.-S. Bres, J. M. C. Boggio, P. A. Andrekson, M. Karlsson, and S. Radic, "Bandwidth-efficient phase modulation techniques for stimulated Brillouin scattering suppression in fiber optic parametric amplifiers," *Opt. Express* **18**(17), 18138–18150 (2010).
12. J. O. White, M. Harfouche, J. Edgecombe, N. Satyan, G. Rakuljic, V. Jayaraman, C. Burgner, and A. Yariv, "1.6 kW Yb fiber amplifier using chirped seed amplification for stimulated Brillouin scattering suppression," *Appl. Opt.* **56**(3), B116–B122 (2017).
13. A. Vasilyev, E. Petersen, N. Satyan, G. Rakuljic, A. Yariv, and J. O. White, "Coherent power combining of chirped-seed Erbium-doped fiber amplifiers," *IEEE Photonics Technol. Lett.* **25**(16), 1616–1618 (2013).
14. E. Petersen, Z. Y. Yang, N. Satyan, A. Vasilyev, G. Rakuljic, A. Yariv, and J. O. White, "Stimulated Brillouin scattering suppression with a chirped laser seed: comparison of dynamical model to experimental data," *IEEE J. Quantum Electron.* **49**(12), 1040–1044 (2013).
15. N. Satyan, A. Vasilyev, G. Rakuljic, V. Leyva, and A. Yariv, "Precise control of broadband frequency chirps using optoelectronic feedback," *Opt. Express* **17**(18), 15991–15999 (2009).
16. V. Jayaraman, G. D. Cole, M. Robertson, C. Burgner, D. John, A. Uddin, and A. Cable, "Rapidly swept, ultra-widely-tunable 1060 nm MEMS-VCSELs," *Electron. Lett.* **48**(21), 1331–1333 (2012).
17. A. V. Harish and J. Nilsson, "Optimization of phase modulation with arbitrary waveform generators for optical spectral control and suppression of stimulated Brillouin scattering," *Opt. Express* **23**(6), 6988–6999 (2015).
18. B. M. Anderson, R. Hui, A. Flores, and I. Dajani, "SBS suppression and coherence properties of a flat top optical spectrum in a high power fiber amplifier," *Proc. SPIE* **10083**, 100830V (2017).
19. A. V. Harish and J. Nilsson, "Optimization of phase modulation formats for suppression of stimulated Brillouin scattering in optical fibers," *IEEE J. Sel. Topics in Quantum Elect.* **24**, 5100110 (2018).

20. Fringes occur in the raw triangle chirp spectrum due to the interference stemming from the same frequency occurring at two places in the period. For this reason, the raw spectrum has been smoothed on a very fine scale with a moving average over 69 MHz. This is close to the same averaging that will occur physically, by virtue of the 57.1 MHz Brillouin linewidth.
21. R. W. Boyd, K. Rzaewski, and P. Narum, "Noise initiation of stimulated Brillouin scattering," *Phys. Rev. A* **42**(9), 5514–5521 (1990).
22. D. S. Elliott, R. Roy, and S. J. Smith, "Extracavity laser band-shape and bandwidth modification," *Phys. Rev. A* **26**(1), 12–18 (1982).
23. C. Wang, M. Zhang, X. Chen, M. Bertrand, A. Shams-Ansari, S. Chandrasekhar, P. Winzer, and M. Lončar, "Integrated lithium niobate electro-optic modulators operating at CMOS-compatible voltages," *Nature* **562**(7725), 101–104 (2018).